

## Catalytic Hydrolysis of Phosphate Diesters by Lanthanide(III) Cryptate (2.2.1) Complexes

Soon Jin Oh, Kyong Hwa Song, Dongmok Whang, Kimoon Kim, Tae Hyun Yoon,<sup>†</sup> Hichung Moon,<sup>†</sup> and Joon Won Park\*Department of Chemistry and Center for Biofunctional Molecules,  
Pohang University of Science and Technology, San 31 Hyoja-Dong, Pohang 790-784, KoreaReceived August 9, 1995<sup>⊗</sup>

Lanthanide(III) Cryptate (2.2.1) chlorides (Ln(2.2.1)Cl<sub>3</sub>; Ln = La (**1a**), Ce(**1b**), and Eu(**1c**); (2.2.1) = 4,7,13-, 16,21-pentaoxa-1,10-diazabicyclo[8.8.5]tricosane) are effective for the catalytic hydrolysis of bis(4-nitrophenyl) phosphate. Kinetic studies reveal that the europium(III) complex (**1c**) catalyzes the hydrolysis to produce 6 equiv of 4-nitrophenol with a significant rate ( $k_1 = 1.5 \times 10^{-4} \text{ s}^{-1}$  at 0.40 mM) at pH 8.5 and 50 °C. The catalytic activity of the complexes is increased with decreasing the ionic size, i.e. La < Ce < Eu. While the use of hydrogen peroxide further increase the activity of **1b** ( $k_1 = 1.6 \times 10^{-3} \text{ s}^{-1}$  at 0.40 mM), the presence of molecular oxygen does not affect the activity at all. Crystal of **1a**·CH<sub>3</sub>OH([La(2.2.1)(Cl)<sub>2</sub>](Cl)(CH<sub>3</sub>OH)) belongs to the space group *Pnma* with  $a = 17.072(3) \text{ \AA}$ ,  $b = 19.037(3) \text{ \AA}$ ,  $c = 14.725(2) \text{ \AA}$ ,  $V = 4786(1) \text{ \AA}^3$ ,  $Z = 8$ ,  $D_x = 1.691 \text{ g cm}^{-3}$ ,  $\mu = 21.7 \text{ cm}^{-1}$ . The cryptated metal ion is nine-coordinated, and all the heteroatoms of the cryptate (2.2.1) ligand coordinate the metal center to form a bowl-shaped structure. Two coordinating chloride anions are located on the open face with a cis geometry. The existence of coordinated water to the europium(III) complex **1c** in the aqueous solution was confirmed by time-resolved Eu(III) luminescence spectroscopy. From the decay constants in H<sub>2</sub>O and D<sub>2</sub>O, the numbers of coordinated water molecules ( $q$ ) are found to be 3.02 at pH of 5.0. The above kinetic and spectroscopic observation are supportive of mechanisms in which the metal complexes act as a center for binding and activation as well as a source of nucleophilic metal hydroxides.

## Introduction

In order to create artificial nucleases, which will overcome shortcomings of the natural ones, a metal center capable of hydrolyzing the phosphate diester of DNA at a reasonable rate has to be connected to a molecular segment recognizing specific base sequences.<sup>1</sup> While considerable progress has been made in developing molecules with sequence-specific recognizing capability, metal complexes featuring high hydrolytic activity for DNA and RNA are currently being actively investigated.<sup>2</sup>

Significant promotion of the hydrolysis of phosphodiester has been achieved mainly with transition metal complexes<sup>3</sup> such as cobalt(III) polyamine complexes,<sup>4</sup> copper(II) complexes,<sup>5</sup> zinc(II) macrocyclic polyamine complexes,<sup>6</sup> and iridium(III) complex.<sup>7</sup> Recently, high reactivity of lanthanide(III) ions and several complexes is demonstrated.<sup>8,9</sup> Obviously, the

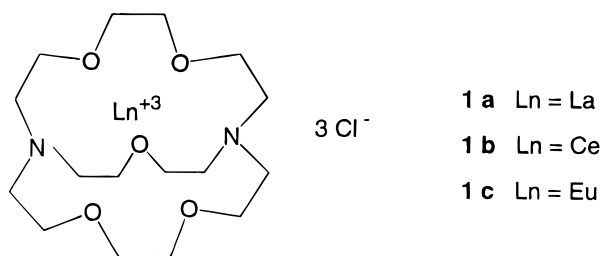
enhanced activity reflects its inherent beneficiary features. For examples, lanthanide(III) macrocyclic complexes have been found to catalyze the hydrolysis of phosphate diesters including RNA.<sup>9c-e</sup> Also, by tethering the macrocyclic ligands to the sequence-specific oligomers hydrolytic cleavage of RNA in a sequence-specific manner has been demonstrated.<sup>10</sup> For this purpose designing macrocyclic ligands which not only form stable complexes with the labile lanthanide ions but also maintain the desirable properties of the metal ions is of utmost importance.

<sup>†</sup> Department of Chemistry, Korea Advanced Institute of Science and Technology, Taejon 305–701, Korea.

<sup>⊗</sup> Abstract published in *Advance ACS Abstracts*, May 15, 1996.

- (1) (a) Bashkin, J. K.; Jenkins, L. A. *Comments Inorg. Chem.* **1994**, *16*, 77–93. (b) Sigman, D. A.; Bruce, T. W.; Mazumder, A.; Sutton, C. L. *Acc. Chem. Res.* **1993**, *26*, 98–104. (c) Chin, J. *Acc. Chem. Res.* **1991**, *24*, 145–152. (d) Hendry, P.; Sargeson, A. M. In *Progress in Inorganic Chemistry*; Lippard, S. J., Ed.; John Wiley & Sons: New York, 1990; Vol. 38, pp 201–258. (e) Uhlenbeck, O. C. *Nature* **1987**, *328*, 596–600. (f) Westheimer, F. H. *Science* **1987**, *235*, 1173–1178. (g) Sigman, D. S. *Acc. Chem. Res.* **1986**, *19*, 180–186. (h) Westheimer, F. H. *Pure Appl. Chem.* **1977**, *49*, 1059–1067.
- (2) The catalytic hydrolysis of RNA is under active research. For these activities, see: (a) Linkletter, B.; Chin, J. *Angew. Chem. Int. Ed. Engl.* **1995**, *34*, 472–474. (b) Amin, S.; Morrow, J. R.; Lake, C. H.; Churchill, M. R. *Angew. Chem. Int. Ed. Engl.* **1994**, *33*, 773–775. (c) Hayashi, N.; Takeda, N.; Shiiba, T.; Yashiro, M.; Watanabe, K.; Komiyama, M. *Inorg. Chem.* **1993**, *32*, 5899–5900. (d) Kolasa, K. A.; Morrow, J. R.; Sharma, A. P. *Inorg. Chem.* **1993**, *32*, 3983–3984. (e) Morrow, J. R.; Buttrey, L. A.; Shelton, V. M.; Berback, K. A. *J. Am. Chem. Soc.* **1992**, *114*, 1903–1905. (f) Modak, A. S.; Gard, J. K.; Merriman, M. C.; Winkler, K. A.; Bashkin, J. K.; Stern, M. K. *J. Am. Chem. Soc.* **1991**, *113*, 283–29. (g) Yoshinari, K.; Yamazaki, K.; Komiyama, M. *J. Am. Chem. Soc.* **1991**, *113*, 5899–5901. (h) Stern, M. K.; Bashkin, J. K.; Sall, E. D. *J. Am. Chem. Soc.* **1990**, *112*, 5357–5359.
- (3) (a) Kim, N.; Suh, J. *J. Org. Chem.* **1994**, *59*, 1561–1571. (b) Weijnen, J. G. J.; Engbersen, J. F. *J. Recl. Trav. Chim. Pays-Bas* **1993**, *112*, 351–357. (c) Browne, K. A.; Bruce, T. C. *J. Am. Chem. Soc.* **1992**, *114*, 4951–4958. (d) De Rosch, M. A.; Trogler, W. C. *Inorg. Chem.* **1990**, *29*, 2409–2416.
- (4) (a) Kim, J. H.; Chin, J. *J. Am. Chem. Soc.* **1992**, *114*, 9792–9795. (b) Chung, Y.; Akkaya, E. U.; Venkatachalam, T. K.; Czarnik, A. W. *Tetrahedron Lett.* **1990**, *31*, 5413–5416. (c) Chin, J.; Banaszczyk, M.; Jubian, V.; Zou, X. *J. Am. Chem. Soc.* **1989**, *111*, 186–190. (d) Chin, J.; Zou, X. *J. Am. Chem. Soc.* **1988**, *110*, 223–225. (e) Rawji, G. H.; Milburn, R. M. *Inorg. Chim. Acta* **1988**, *150*, 227–232.
- (5) (a) Wall, M.; Resemary, C. H.; Chin, J. *Angew. Chem. Int. Ed. Engl.* **1993**, *32*, 1633–1635. (b) Morrow, J.; Trogler, W. C. *Inorg. Chem.* **1988**, *27*, 3387–3394.
- (6) (a) Shionoya, M.; Kimura, E.; Shiro, M. *J. Am. Chem. Soc.* **1993**, *115*, 6730–6737. (b) Koike, T.; Kimura, E.; Nakamura, I.; Hashimoto, Y.; Shiro, M. *J. Am. Chem. Soc.* **1992**, *114*, 7338–7345. (c) Koike, T.; Kimura, E. *J. Am. Chem. Soc.* **1991**, *113*, 8935–8941.
- (7) Hendry, P.; Sargeson, A. M. *J. Am. Chem. Soc.* **1989**, *111*, 2521–2527.
- (8) Breslow, R.; Huang, D.-L. *Proc. Natl. Acad. Sci. U.S.A.* **1991**, *88*, 4080–4083.
- (9) (a) Takasaki, B. K.; Chin, J. *J. Am. Chem. Soc.* **1994**, *116*, 1121–1122. (b) Sumaoka, J.; Miyama, S.; Komiyama, M. *J. Chem. Soc., Chem. Commun.* **1994**, 1755–1756. (c) Breslow, R.; Zhang, B. *J. Am. Chem. Soc.* **1994**, *116*, 7893–7894. (d) Amin, S.; Morrow, J. R.; Lake, C. H.; Churchill, M. R. *Angew. Chem., Int. Ed. Engl.* **1994**, *33*, 773–775. (e) Schneider, H.-J.; Rammo, J.; Hettich, R. *Angew. Chem., Int. Ed. Engl.* **1993**, *32*, 1716–1719. (f) Takasaki, B. K.; Chin, J. *J. Am. Chem. Soc.* **1993**, *115*, 9337–9338.
- (10) (a) Magda, D.; Miller, R. A.; Sessler, J. L.; Iverson, B. L. *J. Am. Chem. Soc.* **1994**, *116*, 7439–7440. (b) Matsumura, K.; Endo, M.; Komiyama, M. *J. Chem. Soc., Chem. Commun.* **1994**, 2019–2020.

Schneider et al. proved that  $\text{Eu}^{+3}$  in combination with a [2,2,2] cryptand is particularly promising. We also reported that lanthanide(III) cryptate (2.2.1) complexes (**1a–c**)<sup>11</sup> can catalyze the hydrolysis of phosphate monoester and triester.<sup>12</sup> Here we



wish to report spectroscopic characterization of the complexes in aqueous and solid phases as well as catalytic activity for the hydrolysis of bis(4-nitrophenyl) phosphate (BNPP).

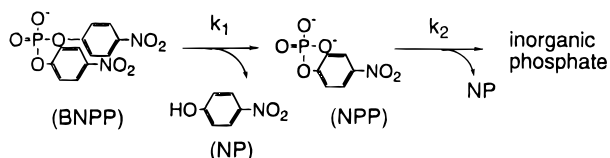
### Experimental Section

**General.** All the chemicals are purchased from Aldrich Chemical Co. and Strem Chemical Co. otherwise mentioned. The lanthanide cryptate (2.2.1) complexes were synthesized under anhydrous conditions.<sup>13</sup> These hygroscopic compounds were handled and weighed in an  $\text{N}_2$ -filled glovebox. Kinetic traces were recorded on a Perkin-Elmer Lambda 15 UV-vis spectrophotometer equipped with a temperature-controlled cell holder.  $^1\text{H}$ - and  $^{31}\text{P}$ -NMR spectra were recorded on a Bruker AM300 spectrometer operating at 300 and 121 MHz, respectively. Infrared spectra were recorded on a Bomem MB-102 FT-IR spectrometer.

**Kinetic Measurement.** Buffers were made up from TRIS (Sigma) or BIS-TRIS (Sigma) and the standardized HCl and NaOH in deionized water (18  $\text{M}\Omega/\text{cm}$ ). Concentration of the buffers is fixed at 0.010 M. The ionic strength of the buffers was maintained at 0.100 M (NaCl). The pH of the buffers was measured at 25 °C with a Corning M220 pH meter fitted with Corning 4765030 combination electrodes. The concentration of the BNPP was fixed at  $4.00 \times 10^{-5}$  M except for the experiments for turnover numbers and concentration effect. A solution of the metal complexes was syringed into a thermostated cell containing BNPP solution. The solution was mixed rapidly, and the absorbances at 400 nm were recorded automatically at intervals of preset time. For the hydrolysis under argon atmosphere, the solutions are completely degassed through freeze-pump-thaw cycles, filled with purified argon, and finally mixed in a closed UV-vis cell designed for handling the air sensitive compounds.

**X-ray Crystallography.** A crystal of the lanthanum(III) complex **1a**- $\text{CH}_3\text{OH}$  was obtained when diethyl ether was allowed to diffuse into the methanolic solution in a Schlenk flask. A colorless crystal ( $0.5 \times 0.4 \times 0.4$  mm) sealed in a Lindemann capillary tube was mounted on an Enraf-Nonius CAD4 diffractometer. A total of 4688 unique reflections having  $2\theta < 50.0^\circ$  were collected by using graphite monochromated  $\text{Mo K}\alpha$  radiation and  $0.75^\circ$ -wide  $\omega$  scans at room temperature. The intensity data were corrected for Lorentz and polarization effects and empirical absorption corrections (DIFABS) were also applied. The structure was solved by a combination of Patterson and difference Fourier methods using SHELXS86 and refined by a full-matrix least-squares method. All the non-hydrogen atoms were refined anisotropically. The positions of hydrogen atoms were idealized

### Scheme 1. Sequential Hydrolysis of Bis(4-nitrophenyl) Phosphate



$$[\text{NP}] \text{ from the first step of the hydrolysis} =$$

$$\text{consumed BNPP} = [\text{BNPP}]_0 - [\text{BNPP}]_t =$$

$$A_0 - A_0 \exp(-k_1 t) \quad (1)$$

$$[\text{NP}] \text{ from the second step of the hydrolysis} =$$

$$[\text{inorganic phosphate}] = A_0 \{1 +$$

$$[k_2 \exp(-k_1 t) - k_1 \exp(-k_2 t)] / (k_1 - k_2)\} \quad (2)$$

$$\text{total } [\text{NP}] = [\text{NP}] \text{ from the first and the second steps} =$$

$$[A_0 - A_0 \exp(-k_1 t)] + A_0 \{1 +$$

$$[k_2 \exp(-k_1 t) - k_1 \exp(-k_2 t)] / (k_1 - k_2)\} \quad (3)$$

( $d(\text{C}-\text{H}) = 0.95 \text{ \AA}$ ) with isotropic thermal parameters of 1.2 times that of attached atoms and included in the calculations of the structure factors as fixed contributions. The refinement converged to  $R(F) = 0.045$ ,  $R_w(F) = 0.051$  where  $w = 4(F_o)^2 / [\sigma(F_o)]^2$  for 2962 observations ( $I > 3\sigma(I)$ ) and 262 variables. The electron density for the highest peak in the final difference map was  $1.78 \text{ e}\cdot\text{\AA}^{-3}$ . All calculations except for the structure-solving were performed with an Enraf-Nonius MOLEN program package.

**Luminescence Spectroscopy.** Solutions of **1c** ( $c = 2.0$  mM) were prepared by dissolving appropriate amount of the sample in doubly deionized  $\text{H}_2\text{O}$  and  $\text{D}_2\text{O}$  (99.9 atom %). The pH of the solutions was measured by using a glass electrode coupled to a digital pH meter (Metrohm Type 632). No correction was applied to the pH values measured in  $\text{D}_2\text{O}$  solution. All luminescence measurements were acquired with the laser spectroscopic system described previously.<sup>14</sup>

### Results and Discussion

**Preparation of the Catalysts.** The lanthanide complexes are prepared in anhydrous methanol from lanthanide chlorides and cryptate (2.2.1) as described in the literatures. A step of recrystallization produces pure products (average yield = 50%). Analysis of the samples with  $^1\text{H}$ -NMR and FT-IR spectroscopy confirmed their high purity.

**Kinetic Studies.** When a buffer solution of the metal complexes was mixed with a solution of BNPP, increase of absorbance at 400 nm was immediate due to formation of 4-nitrophenol (NP). When a large excess of sodium acetate was added to quench the free lanthanide ions,<sup>15</sup> no sign of retardation of the hydrolytic activity is observed. This observation and the unique reactivity pattern (*vide infra*) strictly eliminate the possibility that the free lanthanide ions are interfering in the reactivity.

The hydrolysis of BNPP generates 4-nitrophenol and 4-nitrophenyl phosphate (NPP); the latter in turn transformed itself into the mixture of inorganic phosphate and 4-nitrophenol (Scheme 1). In most cases the rate of the second step is much faster than that of the first one. Therefore, for these particular cases production of 2 equiv of 4-nitrophenol at a rate constant  $k_1$  can be assumed. However, this is not the case for the lanthanide(III) cryptate complexes. The rate of the second step

(11) The full name of cryptate (2.2.1) is 4,7,13,16,21-pentaoxa-1,10-diazabicyclo[8.8.5]tricosane. We chose the particular type of cryptate, because  $\text{Eu}(2.2.2)^{+3}$  is unstable against decomplexation in aqueous buffers, but  $\text{Eu}(2.2.1)^{+3}$  is stable enough to behave as an efficient molecular catalyst.<sup>12</sup> For general information on lanthanide macrocyclic complexes, see: (a) Adachi, G. Y.; Hirashima, Y. In *Cation Binding by Macrocycles*; Inoue, Y., Gokel, G. W., Eds.; Marcel Dekker: New York, 1990; pp 701–741. (b) Bünzli, J.-C.; Wessner, D. *Coord. Chem. Rev.* **1984**, *60*, 191–253.

(12) (a) Oh, S. J.; Song, K. H.; Park, J. W. *J. Chem. Soc., Chem. Commun.* **1995**, 575–576. (b) Oh, S. J.; Yoon, C. W.; Park, J. W. *J. Chem. Soc., Perkin Trans. 2* **1996**, 329–331.

(13) Almasio, M.-C.; Arnaud-Neu, F.; Schwing-Weill, M.-J. *Helv. Chim. Acta* **1983**, *66*, 1296–1306.

(14) Yoon, T. H.; Moon, H.; Park, Y. J.; Park, K. K. *Environ. Sci. Technol.* **1994**, *28*, 2139–2146.

(15) From the control experiments, the free lanthanide ions show comparable reactivity, but the reactivity is reduced significantly by addition of sodium acetate at the controlled pH.

**Table 1.** pH Dependence of the Rate Constants ( $k_2$ ) at 50 °C ([NPP] =  $4.0 \times 10^{-5}$  M; [I] =  $4.0 \times 10^{-4}$  M)

catalyst	pH	$k_2, s^{-1}$
<b>1a</b>	8.5	$5.3 \times 10^{-5}$
<b>1b</b>	8.5	$6.6 \times 10^{-5}$
<b>1c</b>	8.5	$1.1 \times 10^{-4}$
<b>1c</b>	8.0	$7.3 \times 10^{-5}$
<b>1c</b>	7.5	$2.4 \times 10^{-5}$
<b>1c</b>	7.0	$1.4 \times 10^{-5}$

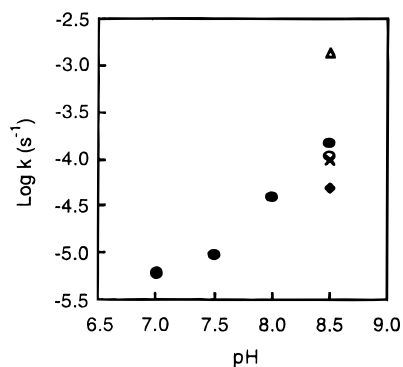
**Table 2.** Change of the Absorbance with Time and Rate Constant ( $k_1$ ) for the Hydrolysis of Bis(4-nitrophenyl) Phosphate in the Presence of Eu(2.2.1)Cl<sub>3</sub> (**1c**) at pH 8.5 and 50 °C ([BNPP] =  $4.0 \times 10^{-5}$  M; [Ic] =  $4.0 \times 10^{-4}$  M;  $k_2 = 1.6 \times 10^{-4} s^{-1}$ )

time, min	absorbance	[NP], $10^{-5}$ M	$k_1, 10^{-4} s^{-1}$
20	0.123	0.75	1.60
40	0.244	1.48	1.65
60	0.353	2.14	1.66
80	0.451	2.73	1.65
100	0.537	3.25	1.62
120	0.614	3.72	1.60
140	0.684	4.15	1.58

**Table 3.** pH Dependence of the Rate Constants ( $k_1$ ) at 50 °C ([BNPP] =  $4.0 \times 10^{-5}$  M; [I] =  $4.0 \times 10^{-4}$  M)

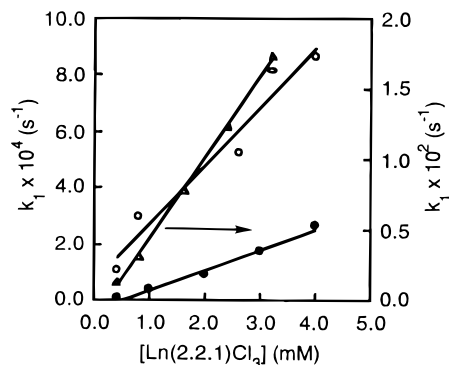
catalyst	pH	$k_1, s^{-1}$
<b>1a</b>	8.5	$5.0(1) \times 10^{-5}$
<b>1b</b>	8.5	$1.1(1) \times 10^{-4}$
<b>1b/H<sub>2</sub>O<sub>2</sub><sup>a</sup></b>	8.5	$1.6(2) \times 10^{-3}$
<b>1b/Ar<sup>b</sup></b>	8.5	$1.0(1) \times 10^{-4}$
<b>1c</b>	8.5	$1.6(1) \times 10^{-4}$
<b>1c</b>	8.0	$4.5(6) \times 10^{-5}$
<b>1c</b>	7.5	$9.3(7) \times 10^{-6}$
<b>1c</b>	7.0	$6.0(8) \times 10^{-6}$

<sup>a</sup> $k_2 = 2.10 \times 10^{-3} s^{-1}$ . <sup>b</sup> $k_2 = 6.51 \times 10^{-5} s^{-1}$ .

**Figure 1.** pH dependence of the pseudo-first-order rate constants for the hydrolysis of BNPP at 50 °C. For each case, the concentration of excess lanthanide(III) (2.2.1) chlorides is held at  $4.0 \times 10^{-4}$  M. (●) **1c**; (Δ) **1b** with 5.0 mM hydrogen peroxide; (○) **1b** in the presence of air; (×) **1b** under argon; (◆) **1a**.

is comparable to that of the first one, which results in a complicated nonlinear kinetic law, i.e., eq 3.<sup>16</sup> The changes of the absorbance at 400 nm and independently measured values of  $k_2$  (Table 1)<sup>12</sup> were applied to the equation. Iteration with a commercial program called Mathematica gives the pseudo-first-order rate constants ( $k_1$ s). Constant  $k_1$  values for each set of data ([NP],  $t$ ) verifies the validity of the eq 3. A typical example of the analysis is shown in Table 2.

The rates were measured at pHs varying from 7.0 to 8.5. The pseudo-first-order rate constants (Table 3) were found to increase with pH of the reaction medium (Figure 1). Because the  $pK_a$  of Eu(2.2.1)<sup>+</sup> is 7.8, at least an edge of plateau should be

**Figure 2.** Effect of concentration of the metal complexes on the pseudo-first-order rate constants: (●) **1c** at pH 7.5; (○) **1b** at pH 8.5; (Δ) **1b** with hydrogen peroxide at pH 8.5.**Table 4.** Effect of Concentration of the Catalyst (**1b**) on the Rate Constants ( $k_1$ ) at pH 8.5 and 50 °C ([BNPP] =  $4.0 \times 10^{-5}$  M)

concn, M	$k_1, s^{-1}$	$k_2, s^{-1}$
$4.0 \times 10^{-4}$	$1.1(1) \times 10^{-4}$	$6.60 \times 10^{-5}$
$8.0 \times 10^{-3}$	$3.0(2) \times 10^{-4}$	$9.73 \times 10^{-5}$
$2.6 \times 10^{-3}$	$5.3(1) \times 10^{-4}$	$2.65 \times 10^{-4}$
$3.2 \times 10^{-3}$	$8.2(2) \times 10^{-4}$	$3.04 \times 10^{-4}$
$4.0 \times 10^{-3}$	$8.7(1) \times 10^{-4}$	$3.73 \times 10^{-4}$

appeared at pH 8.0–8.5 in the pH–rate profile. While this type of plateau was observed for the hydrolysis of 4-nitrophenyl phosphate (NPP), it is not certain at this point why this can not be observed for BNPP. Experimental error might be one of the reasons. Solely with our kinetic data, it is hard to exclude the nucleophilic attack of OH<sup>-</sup>, but reactivities and selectivities of the lanthanide ions and complexes observed by all other workers strongly favors the attack of [M–OH]. Therefore, as in the case for the NPP, the pH dependence of the rate constants can be best rationalized by considering the Brønsted acidity of water molecules bound to the metal centers (*vide infra*). In other word, increasing the pH of the solution will produce deprotonated species (L<sub>n</sub>M–OH), which results in the higher apparent reactivity.

Among complexes **1a–c** the europium complex was shown to have the highest reactivity and the lanthanum(III) complex the lowest reactivity. The order of reactivity is well in accord with the ionic size of the metal ions, which determines the acidity of the bound water ligands.

Hence enhancement of the rate by the use of hydrogen peroxide or molecular oxygen was reported for the lanthanide(III) species;<sup>9a,c,f</sup> application of the method was tried if the same type of enhancement could be attainable with these complexes. When complex **1b** was combined with hydrogen peroxide, the rate of the hydrolysis was enhanced sharply. Meanwhile, the addition of peroxide does not enhance the reactivity of complexes **1a** and **1c**. The addition only induces faster decomposition of these complexes. Without hydrogen peroxide, the activity of the cerium cryptate complex is of expected order, i.e., La < Ce < Eu. Also it is interesting to notice that the activity of the cerium complex was not enhanced by the presence of molecular oxygen.<sup>9a</sup>

Concentration of the metal complexes was varied to see if saturation of  $k_1$  could be observed. As shown in Figure 2, the rate constants are linearly proportional against the concentration up to 4.0 mM of **1b** and **1c** (Tables 4–6). The results verify that for all of the cases the only one metal center is involved for the hydrolysis. It is interesting to notice the difference between the behavior of the metal complexes and that of cerium ion and hydrogen peroxide; in the latter case the two metal ions are involved as the hydrolytic center.<sup>9f</sup> With 4.0 mM of **1c** a

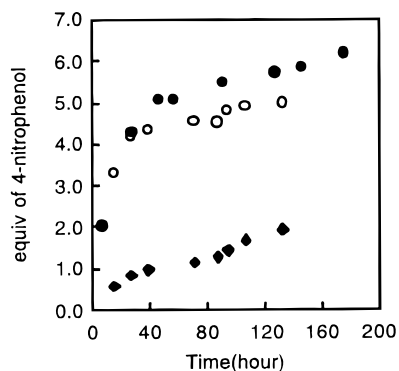


**Figure 3.** Catalytic production of 4-nitrophenol. (◆) **1a**; (○) **1b**; (●) **1c** at pH 8.5 and 50 °C. Forty equimolar concentration of BNPP ( $4.0 \times 10^{-3}$  M) was employed for the experimental runs.

**Table 5.** Effect of Concentration of the Catalyst (**1b**) in the Presence of Hydrogen Peroxide at pH 8.5 and 50 °C ([BNPP] =  $4.0 \times 10^{-5}$  M; [H<sub>2</sub>O<sub>2</sub>] =  $5 \times 10^{-3}$  M)

concn, M	$k_1, s^{-1}$	$k_2, s^{-1}$
$4.0 \times 10^{-4}$	$1.6(2) \times 10^{-3}$	$2.10 \times 10^{-3}$
$8.0 \times 10^{-4}$	$3.2(4) \times 10^{-3}$	$6.38 \times 10^{-3}$
$1.6 \times 10^{-3}$	$7.9(3) \times 10^{-3}$	$1.83 \times 10^{-2}$
$2.4 \times 10^{-3}$	$1.2(1) \times 10^{-2}$	$3.28 \times 10^{-2}$
$3.2 \times 10^{-3}$	$1.7(2) \times 10^{-2}$	$4.12 \times 10^{-2}$

**Table 6.** Effect of Concentration of the Catalyst (**1c**) on the Rate Constants ( $k_1$ ) at pH 7.5 and 50 °C ([BNPP] =  $4.0 \times 10^{-5}$  M)

concn, M	$k_1, s^{-1}$	$k_2, s^{-1}$
$4.0 \times 10^{-4}$	$9.3(7) \times 10^{-6}$	$2.40 \times 10^{-5}$
$1.0 \times 10^{-3}$	$4.3(5) \times 10^{-5}$	$4.78 \times 10^{-5}$
$2.0 \times 10^{-3}$	$9.2(6) \times 10^{-5}$	$8.22 \times 10^{-5}$
$3.0 \times 10^{-3}$	$1.8(3) \times 10^{-4}$	$1.14 \times 10^{-4}$
$4.0 \times 10^{-3}$	$2.7(5) \times 10^{-4}$	$1.70 \times 10^{-4}$

remarkably high rate constant ( $2.7 \times 10^{-4} s^{-1}$  at pH 7.5) is observed. Therefore, ca.  $10^6$ -fold enhancement of the hydrolysis rate was achieved with 4.0 mM of the europium complex.<sup>17</sup> Moreover, in the presence of hydrogen peroxide the cerium complex shows an even higher rate constant ( $1.7 \times 10^{-2} s^{-1}$  at pH 8.5). It is interesting to notice that the metal complexes are more efficient catalysts for the phosphate diesters than for the phosphate monoesters.<sup>12</sup> The metal complex discriminates dianionic substrates from the monoanionic ones, probably because of larger binding affinity and charge neutralization effect for the former substrates. Outcome of the discrimination is the comparable rate constants for the phosphate monoesters and diesters.

In addition to the enhancement of rates, the catalytic turnover is one of the critical criteria for successful artificial nucleases. As shown in Figure 3, almost 6 equiv of 4-nitrophenol was produced when a 2.5% equimolar amount of the europium(III) complex was applied for the hydrolysis of BNPP at pH 8.5. The analysis of the reaction mixture by <sup>31</sup>P-NMR spectroscopy also showed that most of the 4-nitrophenol originated from the first hydrolysis step. For the europium complex rapid initial hydrolysis and saturation were observed (Table 7). The cerium complex showed similar activity, but the lanthanum complex barely produced 2 equiv of 4-nitrophenol. Reduction of the rate after the initial stage is presumably due to inhibition of products, 4-nitrophenyl phosphate and inorganic phosphate. Decomposition leading to the lanthanide ion will not reduce the rate as much as in Figure 3, because the metal ions themselves are reactive catalysts for the hydrolysis. Also

**Table 7.** Change of Absorbance in the Presence of Excess Substrate at pH 8.5 and 50 °C ([BNPP] =  $4.0 \times 10^{-3}$  M; [**1c**] =  $1.0 \times 10^{-4}$  M)

time, h	absorbance <sup>a</sup>	equiv of NP
7.00	3.384 ( $1.128 \times 3$ )	2.05
27.5	7.104 ( $1.184 \times 6$ )	4.31
46.5	8.370 ( $0.837 \times 10$ )	5.07
57.0	8.400 ( $0.560 \times 15$ )	5.09
90.8	9.060 ( $0.604 \times 15$ )	5.49
127	9.435 ( $0.629 \times 15$ )	5.72
146	5.860 ( $0.645 \times 15$ )	5.86
176	6.200 ( $0.682 \times 15$ )	6.20

<sup>a</sup> The absorbance was measured after each sample was diluted with the buffer solution of the same pH. The data in parenthesis represent the observed absorbance times the dilution factor.

**Table 8.** Selected Bond Lengths and Angles for **1a**·CH<sub>3</sub>OH<sup>a</sup>

La—Cl1	2.824(2)	La—Cl2	2.794(2)	La—O1	2.579(6)
La—O2	2.588(6)	La—O3	2.643(6)	La—O4	2.667(6)
La—O5	2.644(6)	La—N1	2.769(7)	La—N2	2.756(7)
Cl1—La—Cl2	79.8(1)	Cl1—La—O1	135.8(2)	Cl1—La—O2	89.2(1)
Cl1—La—O3	75.8(1)	Cl1—La—O4	135.4(1)	Cl1—La—O5	86.1(1)
Cl1—La—N1	150.5(2)	Cl1—La—N2	77.7(2)	Cl2—La—O1	144.3(2)
Cl2—La—O2	78.7(1)	Cl2—La—O3	132.8(1)	Cl2—La—O4	73.8(1)
Cl2—La—O5	92.3(1)	Cl2—La—N1	86.0(2)	Cl2—La—N2	146.6(2)

<sup>a</sup> Numbers in parentheses are estimated standard deviations in the least significant digits.

**Table 9.** Positional and Equivalent Isotropic Thermal Parameters for **1a**·CH<sub>3</sub>OH<sup>a</sup>

atom	x	y	z	$B_{eq}, \text{Å}^2$
La	0.19850(3)	0.08170(2)	0.03304(3)	2.137(7)
Cl1	0.1788(1)	-0.0517(1)	-0.0478(2)	3.93(5)
Cl2	0.1302(2)	0.1207(1)	-0.1319(2)	3.66(5)
Cl3	0.0395(2)	0.1447(1)	0.3886(2)	4.26(5)
O1	0.2579(4)	0.1286(4)	0.1823(4)	3.6(1)
O2	0.0513(4)	0.0817(3)	0.0753(4)	3.1(1)
O3	0.1510(4)	0.0005(4)	0.1678(4)	3.4(1)
O4	0.2665(4)	0.2022(3)	-0.0154(4)	3.0(1)
O5	0.3407(3)	0.0803(3)	-0.0382(4)	3.2(1)
O11	0.4404(6)	0.2621(6)	0.2124(7)	9.2(3)
N1	0.1361(5)	0.2051(4)	0.1015(5)	2.9(1)
N2	0.3124(4)	0.0030(4)	0.1183(5)	3.2(2)
C1	0.1438(7)	0.2009(5)	0.2024(6)	4.0(2)
C2	0.2266(7)	0.1881(6)	0.2309(6)	4.8(3)
C3	0.3388(8)	0.1134(7)	0.199(1)	8.8(3)
C4	0.3612(6)	0.0446(7)	0.1825(7)	5.3(3)
C5	0.0529(6)	0.2067(5)	0.0749(7)	4.0(2)
C6	0.0079(6)	0.1430(6)	0.1032(8)	4.0(2)
C7	0.0231(6)	0.0178(5)	0.1180(7)	3.3(2)
C8	0.0716(6)	0.0014(5)	0.1996(6)	3.5(2)
C9	0.2069(7)	-0.0337(6)	0.2251(7)	4.7(2)
C10	0.2736(6)	-0.0574(6)	0.1660(7)	4.7(2)
C11	0.1751(6)	0.2698(5)	0.0678(7)	3.8(2)
C12	0.2128(6)	0.2613(5)	-0.0234(7)	3.7(2)
C13	0.3166(6)	0.1953(5)	-0.0937(6)	3.6(2)
C14	0.3778(5)	0.1435(5)	-0.0708(6)	3.4(2)
C15	0.3994(5)	0.0291(5)	-0.0131(6)	3.5(2)
C16	0.3622(5)	-0.0267(5)	0.0445(7)	3.7(2)
C10	10.4159(9)	0.3052(8)	0.139(1)	7.9(4)

<sup>a</sup> The isotropic equivalent displacement parameter is defined as  $(4/3)[a^2B(1,1) + b^2B(2,2) + c^2B(3,3) + ab(\cos \gamma)B(1,2) + ac(\cos \beta)B(1,3) + bc(\cos \alpha)B(2,3)]$ .

because the complexes demonstrate catalytic turnover for the hydrolysis of the first hydrolyzed product, 4-nitrophenylphosphate,<sup>12</sup> the inorganic phosphate must be the major inhibitor.

**X-ray Crystallography.** A crystal of the lanthanum(III) complex **1a**·CH<sub>3</sub>OH was obtained when diethyl ether was allowed to diffuse into the methanolic solution under anhydrous condition. X-ray crystallographic structure (Figure 4) shows that the cryptand ligand and two chloride anions form an inner-

(17) The first-order rate constant for the unactivated hydrolysis of BNPP is  $3.0 \times 10^{-10} s^{-1}$  at pH of 7.0 and 50 °C. See reference 4d.

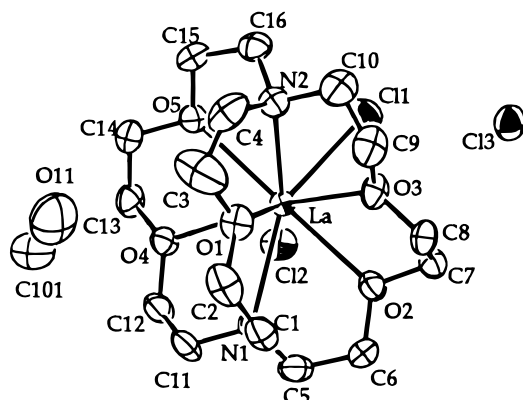


**Figure 4.** ORTEP plot of  $1a \cdot \text{CH}_3\text{OH}$  with labelling scheme.

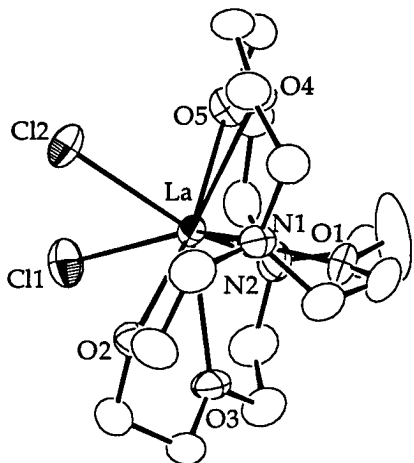


**Figure 5.** ORTEP plot of  $1a \cdot \text{CH}_3\text{OH}$  with hydrogen atoms, non-coordinating methanol, and noncoordinating chloride anion removed for clarity.

sphere complex, and a molecule of methanol fills the space. The encrypted metal ion is nine-coordinated, and all the heteroatoms of the cryptate (2.2.1) ligand coordinate the metal center to form a bowl-shaped structure. Two coordinating chlorides are located on the open face with a *cis* geometry (Figure 5).<sup>18</sup> The novel structure implies that a *cis*-diaqua complex, of which the geometry is suitable for the binary activation of the substrate, can be formed in a buffer solution.

**Luminescence Spectroscopy.** For identification of the Eu(III) species in aqueous media,<sup>20</sup>  $^7\text{F}_0 \rightarrow ^5\text{D}_0$  excitation spectra were obtained as a function of pH (Figure 6). It is clear that there are two types of Eu(III) species in aqueous solution. At low pH a peak of relatively low intensity ( $\lambda_{\text{max}} = 579.87 \text{ nm}$ ) was observed. As the pH of the solution increases, a broad and intense peak centered around 578.63 nm starts to grow. Eventually, only the peak at shorter wavelength was observed at pH of 8.78.

Since there are no ionizable groups in the cryptate (2.2.1) ligand that correspond to the pH range, it can be inferred that the spectral change depending on pH is associated with the bound europium ion, in particular, deprotonation of water molecules coordinated to the metal center.

The lifetimes of  $^5\text{D}_0$  states of the two Eu(III) species were measured in  $\text{H}_2\text{O}$  and  $\text{D}_2\text{O}$ . The number of water molecules bound to the metal ion, i.e., hydration number ( $q$ ) was calculated

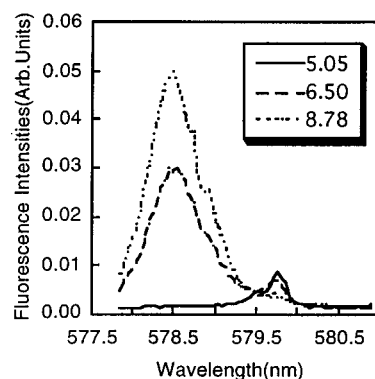
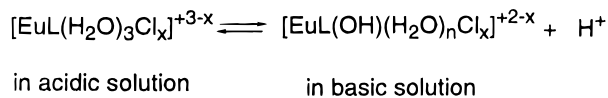


**Figure 6.** Excitation spectra of the Eu(III) complex ( $1c$ ) as a function of pH. The peak at shorter wavelength (578.63 nm) is attributed to the  $\text{Eu}(\text{OH})$  species, while the other peak at 579.87 nm is due to the  $\text{Eu}(\text{OH}_2)$  species. The luminescence was detected through a monochromator set at 616 nm with a band pass of 2.29 nm.

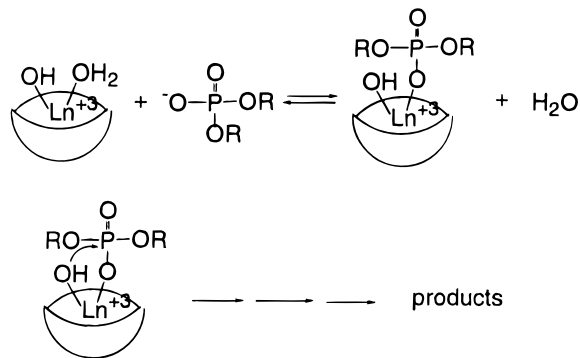
**Table 10.** Excited-State Reciprocal Lifetimes ( $1/\tau$ ) in  $\text{H}_2\text{O}$  and  $\text{D}_2\text{O}$  and Estimated Numbers of Water Molecules ( $q$ ) Coordinated to Eu(2.2.1) Complex ( $1c$ )

pH	$1/\tau_{\text{H}_2\text{O}}, \text{ms}^{-1}$	$1/\tau_{\text{D}_2\text{O}}, \text{ms}^{-1}$	$q$
5.0	5.282	2.402	3.02
8.8	3.042	1.367	1.76

**Scheme 2.** Equilibrium Behavior of the Coordinated Water Molecules



**Scheme 3.** Proposed Mechanism for the Catalytic Hydrolysis of BNPP with the Lanthanide(III) Complexes



from the empirical equation,<sup>19</sup>

$$q = 1.05(1/\tau_{\text{H}_2\text{O}} - 1/\tau_{\text{D}_2\text{O}}) \quad (4)$$

where  $\tau_{\text{H}_2\text{O}}$  and  $\tau_{\text{D}_2\text{O}}$  are lifetimes in  $\text{H}_2\text{O}$  and  $\text{D}_2\text{O}$ , respectively.

At pH 5.0, the hydration number is 3.02 (Table 10), indicating that the molecular formula of the species is  $[\text{Eu}(\text{2.2.1})-(\text{H}_2\text{O})_3\text{Cl}_x]^{+3-x}$ . On the other hand the number at pH 8.8 is 1.76, which suggests that the number of OH vibrating oscillators bound to the Eu(III) ion is reduced. Because water molecules coordinated to Eu(III) ion are expected to be deprotonated under basic conditions, the observed change of the hydration numbers is well in accord with the expectation (Scheme 2).

(18) The crystal structure of Eu(2.2.2.) perchlorate shows that a perchlorate anion acting as a bidentate ligand binds to the metal center. Also it is easily seen that the Eu(2.2.1) complex provides wider open space for incoming substrates. For the crystal structure of Eu(2.2.2) perchlorate, see: Ciampolini, M.; Dapporto, P.; Nardi, N. *J. Chem. Soc. Dalton* **1979**, 974.

(19) Horrocks, W. D.; Sudnick, D. R. *J. Am. Chem. Soc.* **1979**, *101*, 334–340.

(20) For full spectroscopic properties of the complex  $1c$ , see: Sabbatini, N.; Dellonte, S.; Ciano, M.; Bonazzi, A.; Balzani, V. *Chem. Phys. Lett.* **1984**, *107*, 212–216.

**Mechanism.** Based on the molecular geometry inferred from the X-ray analysis and time-resolved luminescence spectroscopy, it can be deduced that the diaquo or triaquo metal complex, in which at least two water ligands are located *cis* to each other, is the major chemical species in aqueous solution. The pH dependence of the excitation spectrum and potentiometric titration<sup>12</sup> clearly shows that one of the water ligands is deprotonated to produce nucleophilic metal hydroxide under basic conditions. This equilibrium behavior can explain the pH dependence of the reactivity of the europium(III) complexes as well as the reactivity order of the three metal complexes. All of the experimental evidence seems to support the “*cis*-diaqua” mechanism (Scheme 3). For the mechanism, demonstrated by Chin et al.,<sup>1c</sup> a bell-shaped pH dependence is expected, but instability of the lanthanide(III) complexes under basic conditions impedes the opportunity to observe such a phenomenon.

A favorable effect of hydrogen peroxide for activity of the cerium(III) complex is evident and is distinct in the sense of molecularity of the metal center. Hydrogen peroxide interacts with the metal center to generate either a Ce(IV) center or a hydroperoxide species (M-OOH). However, at this moment we have no reason to favor a specific mechanism.

### Conclusion

A huge enhancement of the rate and truly catalytic turnover were achieved when the lanthanide(III) (2.2.1) complexes

were applied for the hydrolysis of BNPP. The crystallographic structure, the luminescence spectroscopic results, and the pH dependence of the rates are supportive of the mechanism in which the metal complex acts as a center for binding and activation of the substrate as well as a source of nucleophilic metal hydroxides, which also explains the huge enhancement of rate constants (ca.  $10^6$ -fold at 4.0 mM concentration of the europium complex).<sup>17</sup> In addition, the cerium (2.2.1) complex ( $c = 3.2$  mM) in combination with hydrogen peroxide further enhances the rate up to  $1.7 \times 10^{-2} \text{ s}^{-1}$  at pH 8.5 and 50 °C.

**Acknowledgment.** We are grateful to the Basic Science Research Fund of Pohang University of Science and Technology and the Korea Science and Engineering Foundation (KOSEF) for financial support. Partial support by POSTECH for the X-ray analysis is gratefully acknowledged by K. Kim.

**Supporting Information Available:** Tables S1–S3 listing full experimental details for data collection and refinement, bond distances and bond angles, and anisotropic thermal parameters for **1a**·CH<sub>3</sub>OH (5 pages). Ordering information is given on any current masthead page.

IC9510526